

IEEE TRANSACTIONS ON GEOSCIENCE AND REMOTE SENSING

A PUBLICATION OF THE IEEE GEOSCIENCE AND REMOTE SENSING SOCIETY



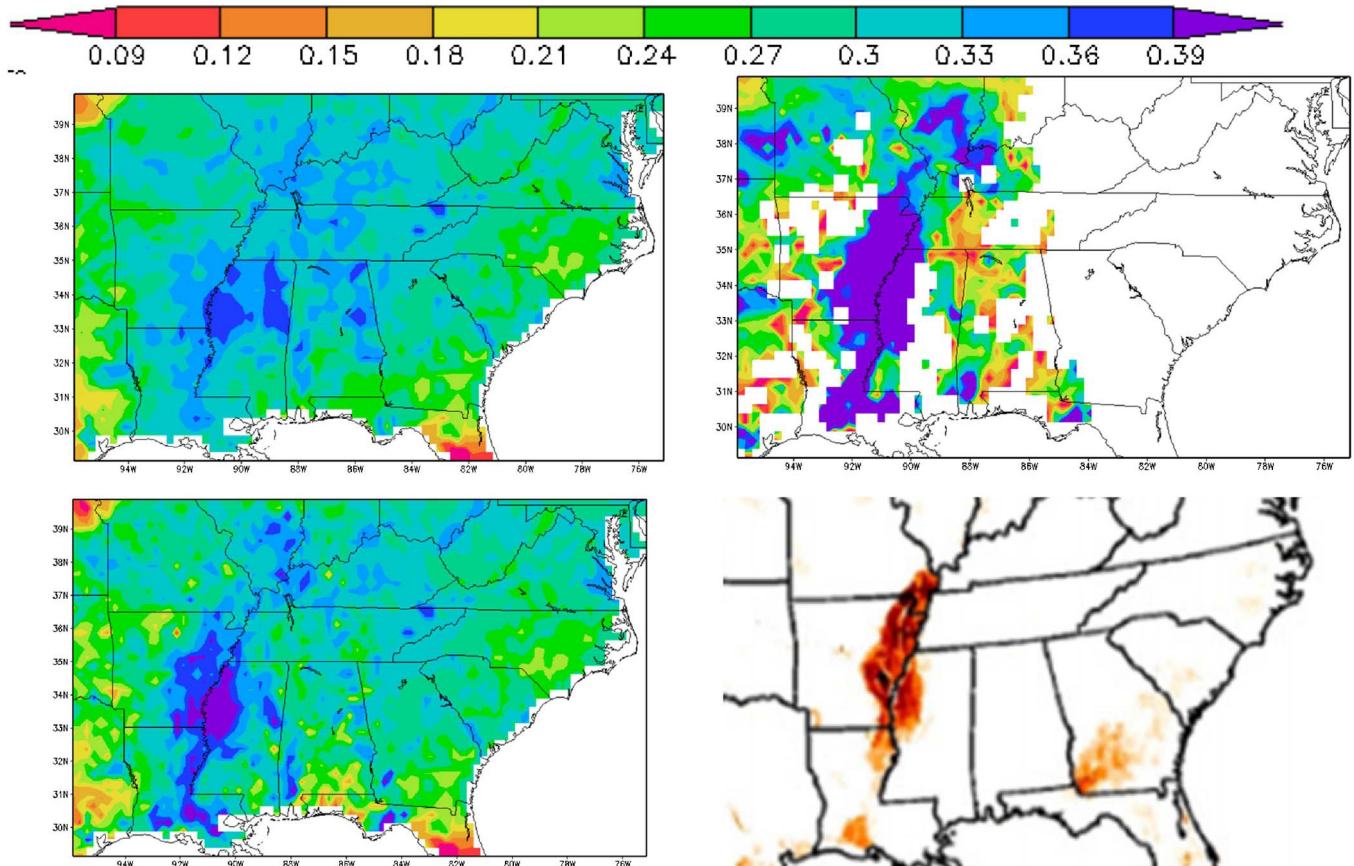
NOVEMBER 2016

VOLUME 54

NUMBER 11

IGRSD2

(ISSN 0196-2892)



Assimilation of SMOS-retrieved soil moisture on 1 April 2013. (Upper left) Noah model surface soil moisture prior to assimilation. (Upper right) SMOS soil moisture. (Lower left) Model analysis after assimilation. Elevated moisture values observed by SMOS may be due to irrigation (lower right).

IEEE TRANSACTIONS ON GEOSCIENCE AND REMOTE SENSING

A PUBLICATION OF THE IEEE GEOSCIENCE AND REMOTE SENSING SOCIETY



NOVEMBER 2016

VOLUME 54

NUMBER 11

IGRSD2

(ISSN 0196-2892)

PAPERS

Atmosphere

- Retrieval and Validation of Atmospheric Aerosol Optical Depth From AVHRR Over China
L. Gao, J. Li, L. Chen, L. Zhang, and A. K. Heidinger 6280

Oceans

- Wave Period and Coastal Bathymetry Using Wave Propagation on Optical Images C. Danilo and F. Melgani 6307
Ocean Color Remote Sensing of Atypical Marine Optical Cases D. D'Alimonte, T. Kajiyama, and A. Saptawijaya 6574

Vegetation and Land

- Measure of Temporal Variation of P-Band Radar Cross Section and Temporal Coherence of a Temperate Tree C. Albinet, P. Borderies, N. Flourey, and E. Pottier 6255
Extending the Pairwise Separability Index for Multicrop Identification Using Time-Series MODIS Images Q. Hu, W. Wu, Q. Song, Q. Yu, M. Lu, P. Yang, H. Tang, and Y. Long 6349
An Iterative BRDF/NDVI Inversion Algorithm Based on *A Posteriori* Variance Estimation of Observation Errors Y. Zeng, J. Li, Q. Liu, A. R. Huete, B. Xu, G. Yin, J. Zhao, L. Yang, W. Fan, S. Wu, and K. Yan 6481
Estimation of Upward Longwave Radiation From Vegetated Surfaces Considering Thermal Directionality T. Hu, Y. Du, B. Cao, H. Li, Z. Bian, D. Sun, and Q. Liu 6644
Modeling and Characteristics of Microwave Backscattering From Rice Canopy Over Growth Stages Y. Liu, K.-S. Chen, P. Xu, and Z.-L. Li 6757

Subsurface and Geology

- Improved Discrimination of Subsurface Targets Using a Polarization-Sensitive Directional Borehole Radar S. Ebihara, T. Kuroda, Y. Koresawa, K. Inada, A. Uemura, and K. Kawata 6429

Electromagnetics

- Radiation of Arbitrary Magnetic Dipoles in a Cylindrically Layered Anisotropic Medium for Well-Logging Applications D. Hong, W.-F. Huang, and Q. H. Liu 6362

(Contents Continued on Page 6254)

Hyperspectral Data Processing	
Blind Hyperspectral Unmixing Using Total Variation and ℓ_q Sparse Regularization	6371
..... J. Sigurdsson, M. O. Ulfarsson, and J. R. Sveinsson	
A Novel Cluster Kernel RX Algorithm for Anomaly and Change Detection Using Hyperspectral Images	6497
..... J. Zhou, C. Kwan, B. Ayhan, and M. T. Eisemann	
Multiple Kernel Learning Based on Discriminative Kernel Clustering for Hyperspectral Band Selection	6516
..... J. Feng, L. Jiao, T. Sun, H. Liu, and X. Zhang	
Nonnegative-Matrix-Factorization-Based Hyperspectral Unmixing With Partially Known Endmembers	6531
..... L. Tong, J. Zhou, Y. Qian, X. Bai, and Y. Gao	
Fast Three-Dimensional Empirical Mode Decomposition of Hyperspectral Images for Class-Oriented Multitask Learning	6625
A Novel Endmember Bundle Extraction and Clustering Approach for Capturing Spectral Variability Within Endmember Classes	6712
..... T. Uezato, R. J. Murphy, A. Melkumyan, and A. Chlingaryan	
Image Processing and Analysis	
Guided Superpixel Method for Topographic Map Processing	6265
..... Q. Miao, T. Liu, J. Song, M. Gong, and Y. Yang	
A New Cascade Model for the Hierarchical Joint Classification of Multitemporal and Multiresolution Remote Sensing Data	6333
..... I. Hedhli, G. Moser, J. Zerubia, and S. B. Serpico	
Measurements of Waves in Landfast Ice Using Inertial Motion Units	6399
..... J. Rabault, G. Sutherland, B. Ward, K. H. Christensen, T. Halsne, and A. Jensen	
Spatial Downscaling of MODIS Land Surface Temperatures Using Geographically Weighted Regression: Case Study in Northern China	6458
..... S.-B. Duan and Z.-L. Li	
Nonconvex Regularization in Remote Sensing	6470
..... D. Tuia, R. Flamary, and M. Barlaud	
Multitemporal Level-1 β Products: Definitions, Interpretation, and Applications	6545
..... D. Amitrano, F. Cecinati, G. Di Martino, A. Iodice, P.-P. Mathieu, D. Riccio, and G. Ruello	
Spiking Neural Networks for Crop Yield Estimation Based on Spatiotemporal Analysis of Image Time Series	6563
..... P. Bose, N. K. Kasabov, L. Bruzzone, and R. N. Hartono	
Multimodal Remote Sensing Image Registration With Accuracy Estimation at Local and Global Scales	6587
..... M. L. Uss, B. Vozel, V. V. Lukin, and K. Chehdi	
Jointly Informative and Manifold Structure Representative Sampling Based Active Learning for Remote Sensing Image Classification	6803
..... A. Samat, P. Gamba, S. Liu, P. Du, and J. Abuduwaili	
Inversion Methods	
Real-Time NDT-NDE Through an Innovative Adaptive Partial Least Squares SVR Inversion Approach	6818
..... M. Salucci, N. Anselmi, G. Oliveri, P. Calmon, R. Miorelli, C. Reboud, and A. Massa	
Microwave Radiometry	
Distribution of Tropical Deep Convective Clouds From Megha-Tropiques SAPHIR Data	6409
..... N. Mathew, C. Suresh Raju, R. Renju, and T. Antony	
Radar Systems	
Near-Real-Time Detection of Tephra Eruption Onset and Mass Flow Rate Using Microwave Weather Radar and Infrasonic Arrays	6292
..... F. S. Marzano, E. Picciotti, S. Di Fabio, M. Montopoli, L. Mereu, W. Degruyter, C. Bonadonna, and M. Ripepe	
All-Directions Through-the-Wall Radar Imaging Using a Small Number of Moving Transceivers	6415
..... B. Yektakhah and K. Sarabandi	
A Deterministic Sea-Clutter Space–Time Model Based on Physical Sea Surface	6659
..... Z. Xin, G. Liao, Z. Yang, Y. Zhang, and H. Dang	
Estimate of Tidal Constituents in Nearshore Waters Using X-Band Marine Radar Image Sequences	6700
..... Z. Chen, J. Pan, Y. He, and A. T. Devlin	
A New Robust Vital Sign Detection in Complex Environments Using Ultrawideband Radar	6771
..... S. M. A. Tayaranian Hosseini, H. Amindavar, and M. Amirmazlaghany	
Real-Time Underwater Object Detection Based on DC Resistivity Method	6833
..... S.-H. Cho, H.-K. Jung, H. Lee, H. Rim, and S. K. Lee	

Synthetic Aperture Radar	
On the Use of the l_2 -Norm for Texture Analysis of Polarimetric SAR Data	X. Deng and C. López-Martínez 6385
Path Planning for GEO-UAV Bistatic SAR Using Constrained Adaptive Multiobjective Differential Evolution	Z. Sun, J. Wu, J. Yang, Y. Huang, C. Li, and D. Li 6444
A Complete Procedure for Crop Phenology Estimation With PolSAR Data Based on the Complex Wishart Classifier . . . L. Mascolo, J. M. Lopez-Sánchez, F. Vicente-Guilalba, F. Nunziata, M. Migliaccio, and G. Mazzarella 6505	
Wavelet Operators and Multiplicative Observation Models—Application to SAR Image Time-Series Analysis	A. M. Atto, E. Trouvé, J.-M. Nicolas, and T. T. Lê 6606
SAR Observation of Eddy-Induced Mode-2 Internal Solitary Waves in the South China Sea	D. Dong, X. Yang, X. Li, and Z. Li 6674
Adaptive Coherency Matrix Estimation for Polarimetric SAR Imagery Based on Local Heterogeneity Coefficients	S. Yang, Q. Chen, X. Yuan, and X. Liu 6732
Region-Based Change Detection for Polarimetric SAR Images Using Wishart Mixture Models	W. Yang, X. Yang, T. Yan, H. Song, and G.-S. Xia 6746
Maritime Signature Correction With the NRL Multichannel SAR	M. A. Sletten, L. Rosenberg, S. Menk, J. V. Toporkov, and R. W. Jansen 6783
Global Navigation Satellite System	
A Phase-Altimetric Simulator: Studying the Sensitivity of Earth-Reflected GNSS Signals to Ocean Topography	A. M. Semmling, V. Leister, J. Saynisch, F. Zus, S. Heise, and J. Wickert 6791
Lidar Systems	
Rapid Updating and Improvement of Airborne LIDAR DEMs Through Ground-Based SfM 3-D Modeling of Volcanic Features	S. Kolzenburg, M. Favalli, A. Fornaciai, I. Isola, A. J. L. Harris, L. Nannipieri, and D. Giordano 6687
Satellite Systems	
Assimilation of SMOS Retrievals in the Land Information System	C. B. Blankenship, J. L. Case, B. T. Zavodsky, and W. L. Crosson 6320

About the Cover: The cover depicts the assimilation of soil moisture retrievals from the Soil Moisture and Ocean Salinity (SMOS) satellite mission into the Noah land surface model on 1 April 2013. (upper left) 0–10 cm model background soil moisture, prior to any assimilation, (upper right) SMOS retrieved near-surface soil moisture, (lower left) model analysis combining background and observations. The high soil moisture values observed in the Mississippi Valley by SMOS are hypothesized to be the result of irrigation associated primarily with rice agriculture, and corresponds well with a map of known irrigated areas (lower right). For more information, please see “Assimilation of SMOS Retrievals in the Land Information System” by Blankenship *et al.*, which begins on page 6320.